

LETTER TO THE EDITOR

Identification of a dwarf galaxy stream in Gaia, and its possible association with the VPOS structure

Hao Tian^{1,2,*}, Chao Liu^{1,2}, Xiang-Xiang Xue^{1,2}, Dongwei Fan¹, Changqing Luo¹, Jundan Nie¹, Ming Yang¹, Yujiao Yang³, and Bo Zhang¹

¹ National Astronomical Observatories, Chinese Academy of Sciences, Beijing 100101, People's Republic of China

² Institute for Frontiers in Astronomy and Astrophysics, Beijing Normal University, Beijing, 102206, People's Republic of China

³ School of Astronomy and Space Science, University of Chinese Academy of Sciences, Beijing, People's Republic of China

Received September 30, 20XX

ABSTRACT

Low surface density streams are important tracers to study the formation and evolution of the Milky Way. Using the accurate astrometric measurements from Gaia mission, we discover a low surface density stream in the north hemisphere, with length of ~ 110 degree and width of 1.23 kpc. The vertical velocity dispersion perpendicular to the stream is around 22.4 km s^{-1} . The spectral data of member candidate stars from LAMOST and DESI shows a large metallicity range from -1.8 to -0.7 . Based on those properties we claim that the stream is originated from a dwarf galaxy. The median metallicity of $[\text{Fe}/\text{H}] = -1.3$ indicates a massive dwarf galaxy origination with stellar mass around $2.0 \times 10^7 M_{\odot}$, which is comparable with the Fornax dwarf galaxy and smaller than LMC/SMC and Sagittarius. We also find the globular cluster Pyxis is highly associated with the stream in the phase space $E - L_z$ and metallicity. The massive progenitor also suggests that many dwarf galaxies, including massive ones, have been disrupted during their evolution orbiting the Milky Way and left with very low surface density structures. This is important to understand the *missing satellites* problem. The orbit information of the stream shows tight association between its progenitor and the Vast Polar Structure (VPOS), which indicates that the satellites fell into the Milky Way in groups, which brought many globular clusters into the Milky Way.

Key words. Galaxy: halo – Galaxy: structure – (Galaxy:) globular clusters: individual:: Pyxis

1. Introduction

During its formation, the Milky Way accreted and merged many satellites (Johnston et al. 2008). Those tidally stripped stellar systems, such as the globular clusters and dwarf galaxies, will left plenty of stars, which orbit the Milky Way with similar kinematic properties as their progenitors (Helmi 2020). In this way, those stellar streams record the merging history of the Milky Way. Since the discovery of the Sagittarius dwarf galaxy by Ibata et al. (1994) and its tidal stream (Ibata et al. 2001; Majewski et al. 2003), around 200 stellar streams have been found during the last two decades (Mateu et al. 2018; Ibata et al. 2024). Especially with the help of deep photometric surveys such as the SDSS (York et al. 2000), Pan-STARRS1 (Chambers et al. 2016) and DES (Dark Energy Survey Collaboration et al. 2016), plenty of cold streams have been discovered from the field stars with matched filter method (Rockosi et al. 2002; Grillmair & Johnson 2006; Grillmair & Dionatos 2006; Grillmair 2006, 2009; Grillmair et al. 2013; Grillmair 2014; Shipp et al. 2018; Grillmair 2022). With precise proper motions provided by Gaia mission, Malhan & Ibata (2018) developed a powerful method and discovered many thin weak streams, which were previously flooded in the field stars (Malhan et al. 2019). More recently, Tian et al. (2024) tried to remove the nearby field stars and discovered a distant stream around 25 kpc. Moreover, combining the radial velocities (RV) from spectroscopic survey, more diffused substructures are discovered in the phase space

(Koppelman et al. 2018; Yang et al. 2019; Dodd et al. 2023; Malhan & Rix 2024).

What is more interesting is that, many of those merged stellar systems did not fall into the Milky Way completely randomly, but in groups. Now we know that many globular clusters are associated with the Sagittarius system, such as Arp2, Berkeley 29, M 54, NGC 5634, Pal 12, Terzan 7, Terzan 8, and Whiting-1 (Bellazzini et al. 2008; Carballo-Bello et al. 2014; Dinescu et al. 2000; Martínez-Delgado et al. 2002; Massari et al. 2019; Nie et al. 2022; Vasiliev 2019). With kinematic information, Massari et al. (2019) studied the formation of the globular clusters in the Milky Way. They found 35% globular clusters were associated with merging events during the formation of the Milky Way. For those dwarf galaxies, it shows that many of them are located in a very thin plane, which is almost perpendicular to the Galactic disk plane. That is also proved with the kinematic information. What is more, Pawlowski et al. (2012) showed that many young halo clusters and streams are also associated with a correlated population, which is a vast structure composed by many dwarf galaxies orbiting in a common polar plane, known as the Vast Polar Structure (VPOS). However, the nature of this structure remains debated. Riley & Strigari (2020) examined the orbit normals of globular clusters and stellar streams and found no evidence of significant clustering.

To study the assemble history of the Milky Way with those streams, the spectroscopic observations are necessary. The spectroscopic surveys, such as LAMOST (Liu et al. 2020), APOGEE (Wilson et al. 2019), S⁵ (Li et al. 2019), H3 (Conroy et al. 2019)

* tianhao@nao.cas.cn

etc., have been proposed to observe the member stars of those known streams to obtain the chemical information and radial velocities. Combining with the proper motions from Gaia, Naidu et al. (2020) reconstructed the formation history of the halo, and found that the Gaia-Sausage-Enceladus (Helmi et al. 2018) dominated the inner halo with galactocentric distance $r < 25$ kpc, while the Sagittarius system dominated the outer part. What is more interesting is that, more than 95% of their samples are linked to the merging substructures, which indicates that the halo has been built by merged dwarf galaxies and the disk heating. Their results proved again that the outer halo was highly structured.

As a result, a key question is that if all the satellites have been discovered. Koposov et al. (2008) showed that the luminosity function of the satellites can be described by a single power law, ranging from $M_V = -2$ to the luminosity of the Large Magellanic Cloud. However, the number of currently discovered satellites is much less than that predicted by the simulations, as known as the *missing satellites* problem (Klypin et al. 1999). One of the possible explanations is that part of those missing satellites have been fully disrupted. In this way, there should be plenty of remnants, such as diffuse streams or clouds, left in the Milky Way. The Orphan stream is an example that many studies prefer its origination from an ultra-faint dwarf galaxy (Grillmair 2006; Sales et al. 2008). It is important to discover those merging events, especially those originated from merged dwarf galaxies with low surface density. However, current methods have strong limitations on the discovery of those faint substructures.

To this end, we focus on those fainter ones or those with low surface densities, which are possibly ignored or difficult to discover in previous work. We apply the similar method of Tian et al. (2024) to Gaia DR3 and discover a new long stream. This paper is constructed as follows. We briefly introduce the data selection and the method in Section 2. The properties of the new stream are introduced in the Section 3. Finally, we summarize the results in the Section 4.

2. Data and Method

In a small sky coverage, the stream member stars will have similar distance and velocities because all of them share unique orbit. Then those member stars will be in form of overdensities on the sky within corresponding proper motion ranges. The challenge is that low number of the member stars will make the stream flooded in the field stars. Thus a very efficient way is needed to remove the contaminations of the field stars, especially those disk stars, which are a few orders higher than that of the halo in number density. This will significantly enhance the signal of the streams (Tian et al. 2024).

Following Tian et al. (2024), we use the data from Gaia DR3 to reveal the substructures in the halo. Here we briefly introduce the steps. Focusing on the substructures in the halo, especially those at high latitude, we firstly select the stars with following criteria.

1. $\omega < 0.1$ mas
2. $\sigma_{\mu_\alpha^*} < 0.2$ mas yr⁻¹ and $\sigma_{\mu_\delta} < 0.2$ mas yr⁻¹
3. RUWE < 1.2

where ω is the parallax, σ_α^* and σ_δ are the uncertainties of the proper motions, and RUWE is the Renormalised Unit Weight Error.

The first criterion removes most of the nearby stars. But a small fraction of distant stars with larger uncertainties of the

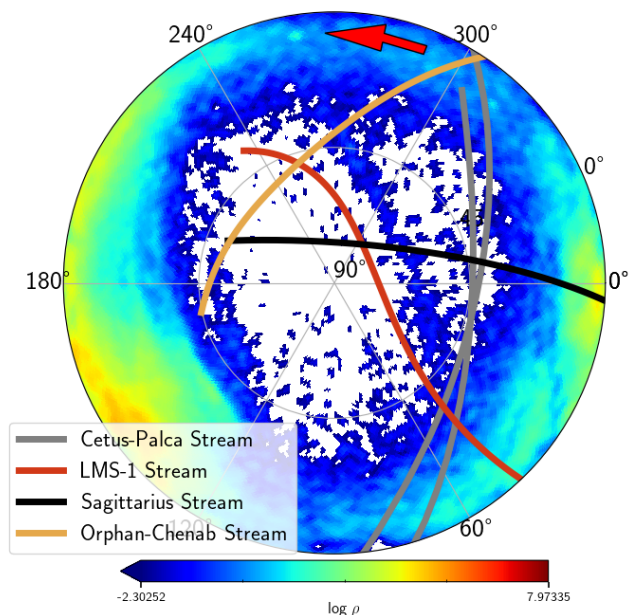


Fig. 1: The density distribution of the selected stars over the north semisphere. **The orbits of four streams are represented by the solid lines, which are provided by Mateu et al. (2018) and Chang et al. (2020).** The globular cluster Pyxis is marked with red arrow with $(l, b) = (261^\circ, 7^\circ)$.

parallax will be also removed. **We do not correct the zero-point of the parallax, which does not affect the final results, because parallax is only used removing the nearby stars.** Assuming the parallax uncertainty is only relative to the magnitude, this will not affect the results, but slightly reduce the number of the member stars, especially those fainter ones. The second criterion ensures the proper measurements of the selected stars are accurate. This will remove most of the fainter stars, i.e. $G > 19$. In this way, those member stars from a unique stream will keep in a smaller range of proper motion. The last criterion is used to make sure that most of the samples are single stars.

3. The new stream

To figure out the substructure candidates, we slice those selected stars according to the proper motions in both α and δ direction, and collect the overdensities on the sky, which are of high probabilities to be a stream.

3.1. Significance

Based on the discussion above, here we report a significant new stellar stream in the north hemisphere with proper motions $0.5 < \mu_{\alpha^*} < 1.5$ mas yr⁻¹ and $-0.5 < \mu_\delta < 0.5$ mas yr⁻¹. Figure 1 shows the density distribution of all the stars satisfying all the selection criteria including the constraints on the proper motions. The new stream candidate is located from top $(l, b) = (270^\circ, 45^\circ)$ to the bottom right, $(l, b) = (30^\circ, 45^\circ)$, which is around 110 degree long. Compared with the stellar stream library galstreams (Mateu et al. 2018), we find that this candidate does not overlap with any previously identified streams in the space, especially those originated from dwarf galaxies, **such as the Orphan Stream (Belokurov et al. 2007; Koposov et al. 2023), the Cetus-Palca Stream (Newberg et al. 2009; Chang et al.**

2020; Yuan et al. 2022), the LMS-1 stream (Yuan et al. 2020; Malhan et al. 2021) as showed in Figure 1.

Following Tian et al. (2024), we also use the package `gala`¹ (Price-Whelan 2017) to rotate the coordinates from equatorial frame to a new one (ϕ_1, ϕ_2) making the stream along the equator in the new frame (ϕ_1, ϕ_2) , i.e. $\phi_2 = 0^\circ$. The stream is around 110 degree long from $\phi_1 = -45^\circ$ to 65° as represented by the shadow region in Figure A.1. Fitting the latitude distribution with a Gaussian distribution, we find the signal-to-noise ratio of the stream is around 19.6. The half width ($1\sigma_{\phi_2}$) is around $2^\circ.57 \pm 0^\circ.52$. The background is around $H = 12.54$ for each latitude bin with size of 1° , which indicates the contamination of the field stars in each bin on average. Then we select all 290 stars within $|\phi_2| < 5^\circ$ (around 2σ) as the member candidates, with around $H * 10$ bins = 125 stars from contamination.

3.2. Geometric property

Cross-matching with the spectroscopic data, we obtain spectra of 22 giant stars in total, 20 stars from LAMOST DR9 and 2 from DESI early data release. The top panel of Figure C.1 shows the distribution of the radial velocity (RV) versus the longitude ϕ_1 of 20 common stars, the other two stars from LAMOST are not showed with RV around -230 km s^{-1} and metallicity lower than -2 . All those 20 common stars are selected as the member candidates to study the properties of the stream. The metallicity of those common stars has a larger variance, from -1.8 to -0.7 , much larger than the uncertainties of ~ 0.1 dex. What should be noticed is that all those common stars are located on the right part of the stream because of the sky coverages of LAMOST and DESI.

First we estimate the metallicity of the stream with the median value of those 20 member stars, $[\text{Fe}/\text{H}] = -1.3$. Then we try to fit the distribution in CMD of all the member stars using the isochrone with metallicity and age $([\text{Fe}/\text{H}], \log_{10} \tau) = (-1.3, 10.08)$. With the package `dustmaps` (Green 2018), we correct the extinction with the dust map obtained by Planck Collaboration et al. (2016) and the extinction coefficients of Gaia bands provided by Wang & Chen (2019), i.e. 2.489, 3.161 and 1.858 for G , B_P and R_P respectively. Then the distance modulus is constrained as $\mathcal{DM} = 17.19$ ($d_{\text{iso}} = 27.42$ kpc). Figure B.1 represents the distributions in CMD of the stars within different longitude ranges from -45° to 65° with step of 22° . The selected common stars with LAMOST and DESI are marked with red and magenta symbols, respectively. From the middle and most right panel, there are two stars significant offset from the fitted isochrone, which are highlighted by the open circle in Figure C.1 and B.1. Those two stars are not considered as member stars of the stream in the following discussion. What should be noticed is that there is no classical distance tracers in the members, such as RR Lyrae stars or blue horizontal branch stars. **So here we adopt the distance $d_{\text{iso}} = 27.42$ kpc for all the member stars.** According to the position of the possible red horizontal branch stars, approximately located at $(B_P - R_P, G) = (0.8, 17.6)$, which is marked with the horizontal dashed line in each panel, there is not significant gradient versus the longitude ϕ_1 . In this way, we firstly estimate the width of the stream by $d_{\text{iso}} * \sigma_{\phi_2} = 1.23$ kpc.

The larger variance of the metallicity and the width discussed above suggest that the stream possibly originates from a dwarf galaxy, rather than a globular cluster.

3.3. Kinematic property

Considering most of the member candidate stars without spectroscopic observation, we only investigate the properties of the tangential velocities, which are perpendicular to the line of sight. The bottom panel of Figure C.1 shows the distribution of the tangential velocities after the correction of all the member candidate stars with $G < 18$. The shadow region represent the ranges caused by the proper motion selection. We find the dispersion of the tangential velocity perpendicular to the stream is around 30.7 km s^{-1} for all those members with $G < 18$. The dispersion is an order higher than that of a cold stellar stream formed from a globular cluster, such as $2.1 \pm 0.3 \text{ km s}^{-1}$ for GD-1 stream (Gialluca et al. 2021). Considering the maximum uncertainties of proper motion, 0.2 mas yr^{-1} , the contribution to the dispersion is $4.74 * d * \sigma_\mu \sim 16.5 \text{ km s}^{-1}$. Assuming a median proper motion of 1 mas yr^{-1} and relative distance uncertainty of 10%, the distance uncertainty will contribute $\sim 13.0 \text{ km s}^{-1}$. Then the intrinsic dispersion can be estimated by $(30.7^2 - 16.5^2 - 13.0^2)^{0.5} = 22.4 \text{ km s}^{-1}$, which is still an order higher than that of the cold stream and almost all the globular clusters³ (Harris 1996, 2010 version). The larger tangential velocity dispersion also suggests that the stream is formed from a disrupted dwarf galaxy. Considering the stream is not orbiting a great circle on the sky, which will enlarge the dispersion of all the member candidates, we also check the dispersion in different longitude ranges as represented by the green symbols, we find the dispersion is still significant enough in each subsample.

3.4. Origination

The large width of 1.23 kpc and the velocity dispersion of 22.4 km s^{-1} indicate the stream is originated from a dwarf galaxy. The stellar mass of its progenitor dwarf galaxy can be estimated as $M_* \sim 2.0 \times 10^7 M_\odot$ with the universal metallicity-mass relation provided by Kirby et al. (2013), adopting the metallicity of -1.3 . That suggests a massive progenitor of dwarf galaxy, which is smaller than the LMC/SMC and the Sagittarius system, and comparable with that of the Fornax spheroidal dwarf galaxy. It is important to note that this relation was derived from dwarf galaxies in the Local Group, with an RMS of 0.17. Meanwhile, the metallicity-mass relation evolves such that higher-redshift galaxies of similar mass tend to be more metal-poor (Erb et al. 2006; Zahid et al. 2013; Henry et al. 2013).

To further investigate its origination, we integrate the orbit of those common stars with full information forward and backward with the package `AGAMA` (Vasiliev 2019) and represent the orbits in Figure 2 with gray lines. The potential of the Milky Way is assumed to be composed by three components, a Dehnen bulge, a Miyamoto-Nagai disk and an NFW halo. The masses for those three parts are $2.0 \times 10^{10} M_\odot$, $5.0 \times 10^{10} M_\odot$ and $5.5 \times 10^{11} M_\odot$, respectively. **The scale radii are set 1.0 kpc, 3.0 kpc and 15.0 kpc, then the total mass enclosed within 20 kpc is around $2.1 \times 10^{11} M_\odot$.** The eccentricity and pericenter distance are of ~ 0.7 and ~ 24 kpc, respectively. The positions of the globular clusters (Vasiliev 2019) and dwarf galaxies (Drlica-Wagner et al. 2020) are also presented by the blue and yellow dots. The LMC and SMC are highlighted with larger yellow

¹ <https://gala.adrian.pw/en/latest/coordinates/greatcircle.html>

² The longitude range is directly relative to the selection of the two points

³ <https://physics.mcmaster.ca/~harris/mwgc.dat>

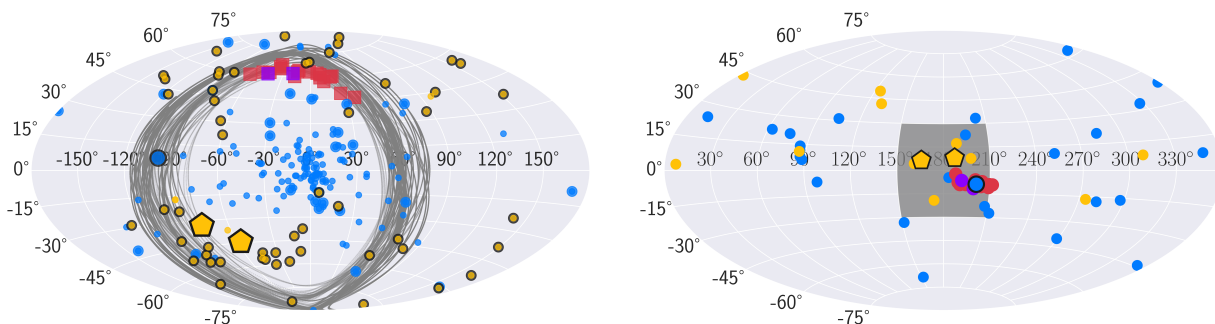


Fig. 2: Left : Sky projection of those common stars, globular clusters and dwarf galaxies represented by the red/magenta squares, blue dots and yellow dots, respectively. The globular cluster Pyxis and LMC/SMC are highlighted with larger blue dot and yellow pentagons. All those globular clusters and dwarf galaxies with distance larger than 20 kpc are highlighted with solid black edge. **The integrated orbits of those stars with full 6D information are represented by the gray lines.** Right: **The direction distribution of those common stars, distant globular clusters and dwarf galaxies with full 6D information are represented.** The symbols are the same with that in the left panel. **The shadow region represents the direction of the normal of the VPOS with longitude between 150° and 210° and latitude between -30° and 30° .**

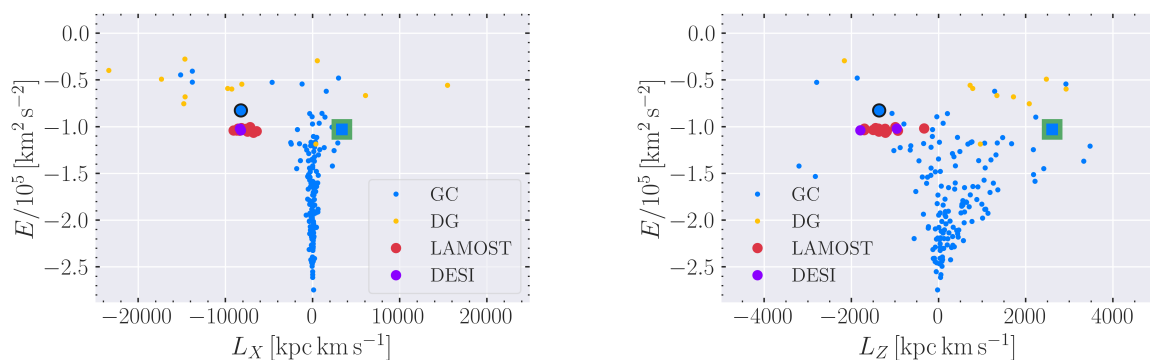


Fig. 3: The distributions of the common stars, the globular clusters and the dwarf galaxies are represented by the red/magenta larger dots, the blue and yellow dots in the phase spaces E versus L_X (left) and L_Z (right), respectively. **The locations of Pyxis and NGC 5824 are highlighted by the larger blue dot and square, respectively.**

low pentagons. **From the sky distribution, we find that many dwarf galaxies and distant globular clusters are located on the orbit of the stream as showed in the left panel of Figure 2.**

This is also proved by the orbit direction distribution in the right panel of Figure 2. We can find two groups, the first one is located around $(0^\circ, 90^\circ)$ where many globular clusters associate with the Sagittarius Stream. The other one is around the direction $(0^\circ, 180^\circ)$, where locates dwarf galaxies associated with the Vast POLar Structure (VPOS) including the LMC, SMC, Carina, Draco, Fornax and Ursa Minor (Pawlowski et al. 2012). The orbit norm directions (direction of the angular momentum vector $\mathbf{L} = (L_X, L_Y, L_Z)$) of those common stars are also located in the similar region around $(\phi, \theta) = (202^\circ.9, -8^\circ.9)$, which indicates an association between the new stream and VPOS.

Checking the phase space distributions of those globular clusters and dwarf galaxies, we find the Pyxis globular cluster is highly associated with the stream as showed in Figure 3. First, it locates on the elongation of the stream. The location of Pyxis is highlighted by the arrow in Figure 1, and by the black-edged blue dot around $(l, b) \sim (-99^\circ, 7^\circ)$ in the left panel in Figure 2. What is more, the stream and Pyxis have similar angular momenta, i.e. the directions of the orbits. Second, Pyxis has a similar metallicity -1.2 (Harris 1996) and CMD distribution. Figure B.1 shows the CMD distribution of the members stars of the stream and the globular cluster Pyxis with black and blue dots, respectively. The members of Pyxis are shifted to the distance of the stream. The extinction of Pyxis from Vasiliev (2019) is

adopted. We find the positions of the red horizontal branch stars are quite consistent. **Meanwhile, we do not find any connection with the Cetus-Palca Stream, which is located mainly in the south semisphere and tightly associated with the globular cluster NGC 5824 (Chang et al. 2020), which is highlighted with square in Figure 3.**

All the evidences above suggest that the stream and the globular cluster Pyxis have the same origination, a dwarf galaxy with stellar mass of $2.0 \times 10^7 M_\odot$. The new stream and the globular cluster Pyxis, are a close analogy as the Sagittarius system or the ω -Centauri system, composed of a stripped stream, and at least one globular cluster and the progenitor dwarf galaxy. What is different is that the new stream has a much larger pericenter distance than the Sagittarius and the ω -Centauri system. That means the tidal effect from the Milky Way is much smaller than that to the Sagittarius and the ω -Centauri system. What should be noticed is that Pyxis is a quite special globular cluster with very large half-light radius, $r_h = 17.7$ pc (Fritz et al. 2017), larger than that of almost all the current discovered globular clusters in the Milky Way and close to the bottom limit of the dwarf galaxies (Drlica-Wagner et al. 2020). The large pericenter distance makes the globular cluster Pyxis survived from the tidal effect of the Milky Way during the disruption of the progenitor dwarf galaxy.

According to the results from Hoyer et al. (2021) based on the analysis of 601 galaxies in the local volume, the occupation of the nuclear star cluster in the galaxies with stellar mass

$< 10^{9.5} M_{\odot}$ can reach up to 40%. More evidence is necessary for further studies on the relation between the globular cluster Pyxis and the progenitor dwarf galaxy, i.e. if Pyxis is the nuclear star cluster or a satellite globular cluster of the progenitor dwarf galaxy, or Pyxis is the remnant of the core of the dwarf galaxy, whose outskirt has been completely stripped. In any case, it is possible that the progenitor dwarf galaxy of the stream has been almost fully disrupted like the ω -Centauri system (Ibata et al. 2019).

The discovery of this new stream suggests again that many globular clusters, especially those relatively metal rich ones, are not formed in the Milky Way, but in those merged dwarf galaxies. Even more, some of those globular clusters are the nuclear star cluster of the stripped galaxies (Zinn 1993; Muratov & Gnedin 2010; Renaud et al. 2017; Drlica-Wagner et al. 2020). Meanwhile the discovery of the new stream also indicate that many dwarf galaxies have been stripped during the evolution of the Milky Way, even those massive ones. This at least partly explains the *missing satellites* problem.

4. Summary

Focusing on the distant volumes, we remove majority of the nearby stars with parallax provided by Gaia DR3. Slicing the proper motions in both directions along α and δ , we find a 110 degree long stellar stream with $0.5 < \mu_{\alpha^*} < 1.5$ and $-0.5 < \mu_{\delta} < 0.5$ mas yr $^{-1}$, which is around ~ 27.42 kpc from the Sun. Through the number fitting along the latitude ϕ_2 perpendicular to the elongation of the stream with a Gaussian profile, we find the half width is around 1.23 kpc (1σ in Gaussian). The tangential velocity dispersion perpendicular to the stream is around 22.4 km s $^{-1}$. The larger width and velocity dispersion indicate an origination from a dwarf galaxy. With the help of LAMOST and DESI, we obtain the full information of 18 stars of high probabilities of stream member. The metallicity $[\text{Fe}/\text{H}] = -1.3$ indicates that the stellar mass of its progenitor is around $2.0 \times 10^7 M_{\odot}$, which is much larger than the majority of the dwarf galaxies in the Milky Way, next to Magellanic system, the Sagittarius and Fornax dwarf galaxies. What is more, the orbits of those stars indicate that this stream is associated with the VPOS. What is more important, we find the globular cluster Pyxis is tightly associated with the new stream. Analogy with the ω -Centauri system, the progenitor dwarf galaxy should have been completely disrupted. It is not clear that if Pyxis is the nuclear star cluster or a satellite globular cluster of the progenitor dwarf galaxy. This discovery proves the path of the formation of the globular clusters in the Milky Way, that many of which are formed from the merged dwarf galaxies. This new discovered stream also indicates that the missed satellites, even massive ones, may have been disrupted during the evolution. Tidal disruption is one of the solutions for the *missing satellites* problem. There should be many low surface density diffuse streams in the halo.

Acknowledgements. We thank the referee for those comments which greatly improved the manuscript. This work is supported by National Key R&D Program of China No. 2024YFA1611902 and the China Manned Space Project. X-X.X. acknowledges the support from CAS Project for Young Scientists in Basic Research Grant No. YSBR-062 and NSFC grants No. 11988101. D.F. acknowledges the support from National Natural Science Foundation of China with Grant No.12273077. J.N. acknowledges the supports by the Beijing Natural Science Foundation (grants No.1232032), by the National Key R&D Program of China (grants No. 2021YFA1600401,2021YFA1600400), by the Chinese National Natural Science Foundation (grants No. 12373019). M.Y. is supported by the National Natural Science Foundation of China (Grant No. 12373048) Y.Y. acknowledges the support from National Natural Science Foundation of China with Grant No.12203064. Data resources are supported by China National Astronomical Data Center (NADC) and Chinese Virtual Observatory (China-VO). This

work is supported by Astronomical Big Data Joint Research Center, co-founded by National Astronomical Observatories, Chinese Academy of Sciences and Alibaba Cloud. This work has made use of data from the European Space Agency (ESA) mission *Gaia* (<https://www.cosmos.esa.int/gaia>), processed by the *Gaia* Data Processing and Analysis Consortium (DPAC, <https://www.cosmos.esa.int/web/gaia/dpac/consortium>). Funding for the DPAC has been provided by national institutions, in particular the institutions participating in the *Gaia* Multilateral Agreement. Guoshoujing Telescope (the Large Sky Area Multi-Object Fiber Spectroscopic Telescope LAMOST) is a National Major Scientific Project built by the Chinese Academy of Sciences. Funding for the project has been provided by the National Development and Reform Commission. LAMOST is operated and managed by the National Astronomical Observatories, Chinese Academy of Sciences.

References

- Bellazzini, M., Ibata, R. A., Chapman, S. C., et al. 2008, *AJ*, 136, 1147
 Belokurov, V., Evans, N. W., Irwin, M. J., et al. 2007, *ApJ*, 658, 337
 Carballo-Bello, J. A., Sollima, A., Martínez-Delgado, D., et al. 2014, *MNRAS*, 445, 2971
 Chambers, K. C., Magnier, E. A., Metcalfe, N., et al. 2016, arXiv e-prints, arXiv:1612.05560
 Chang, J., Yuan, Z., Xue, X.-X., et al. 2020, *ApJ*, 905, 100
 Conroy, C., Bonaca, A., Cargile, P., et al. 2019, *ApJ*, 883, 107
 Dark Energy Survey Collaboration, Abbott, T., Abdalla, F. B., et al. 2016, *MNRAS*, 460, 1270
 Dinescu, D. I., Majewski, S. R., Girard, T. M., & Cudworth, K. M. 2000, *AJ*, 120, 1892
 Dodd, E., Callingham, T. M., Helmi, A., et al. 2023, *A&A*, 670, L2
 Drlica-Wagner, A., Bechtol, K., Mau, S., et al. 2020, *ApJ*, 893, 47
 Erb, D. K., Shapley, A. E., Pettini, M., et al. 2006, *ApJ*, 644, 813
 Fritz, T. K., Linden, S. T., Zivick, P., et al. 2017, *ApJ*, 840, 30
 Gialluca, M. T., Naidu, R. P., & Bonaca, A. 2021, *ApJ*, 911, L32
 Green, G. 2018, *The Journal of Open Source Software*, 3, 695
 Grillmair, C. J. 2006, *ApJ*, 645, L37
 Grillmair, C. J. 2009, *ApJ*, 693, 1118
 Grillmair, C. J. 2014, *ApJ*, 790, L10
 Grillmair, C. J. 2022, *ApJ*, 929, 89
 Grillmair, C. J., Cutri, R., Masci, F. J., et al. 2013, *ApJ*, 769, L23
 Grillmair, C. J. & Dionatos, O. 2006, *ApJ*, 643, L17
 Grillmair, C. J. & Johnson, R. 2006, *ApJ*, 639, L17
 Harris, W. E. 1996, *AJ*, 112, 1487
 Helmi, A. 2020, *ARA&A*, 58, 205
 Helmi, A., Babusiaux, C., Koppelman, H. H., et al. 2018, *Nature*, 563, 85
 Henry, A., Scarlata, C., Domínguez, A., et al. 2013, *ApJ*, 776, L27
 Hoyer, N., Neumayer, N., Georgiev, I. Y., Seth, A. C., & Greene, J. E. 2021, *MNRAS*, 507, 3246
 Ibata, R., Irwin, M., Lewis, G. F., & Stolte, A. 2001, *ApJ*, 547, L133
 Ibata, R., Malhan, K., Tenachi, W., et al. 2024, *ApJ*, 967, 89
 Ibata, R. A., Bellazzini, M., Malhan, K., Martin, N., & Bianchini, P. 2019, *Nature Astronomy*, 3, 667
 Ibata, R. A., Gilmore, G., & Irwin, M. J. 1994, *Nature*, 370, 194
 Johnston, K. V., Bullock, J. S., Sharma, S., et al. 2008, *ApJ*, 689, 936
 Kirby, E. N., Cohen, J. G., Guhathakurta, P., et al. 2013, *ApJ*, 779, 102
 Klypin, A., Gottlöber, S., Kravtsov, A. V., & Khokhlov, A. M. 1999, *ApJ*, 516, 530
 Koposov, S., Belokurov, V., Evans, N. W., et al. 2008, *ApJ*, 686, 279
 Koposov, S. E., Erkal, D., Li, T. S., et al. 2023, *MNRAS*, 521, 4936
 Koppelman, H., Helmi, A., & Veljanoski, J. 2018, *ApJ*, 860, L11
 Li, T. S., Koposov, S. E., Zucker, D. B., et al. 2019, *MNRAS*, 490, 3508
 Liu, C., Fu, J., Shi, J., et al. 2020, arXiv e-prints, arXiv:2005.07210
 Majewski, S. R., Skrutskie, M. F., Weinberg, M. D., & Ostheimer, J. C. 2003, *ApJ*, 599, 1082
 Malhan, K. & Ibata, R. A. 2018, *MNRAS*, 477, 4063
 Malhan, K., Ibata, R. A., Carlberg, R. G., et al. 2019, *ApJ*, 886, L7
 Malhan, K. & Rix, H.-W. 2024, *ApJ*, 964, 104
 Malhan, K., Yuan, Z., Ibata, R. A., et al. 2021, *ApJ*, 920, 51
 Martínez-Delgado, D., Zinn, R., Carrera, R., & Gallart, C. 2002, *ApJ*, 573, L19
 Massari, D., Koppelman, H. H., & Helmi, A. 2019, *A&A*, 630, L4
 Mateu, C., Read, J. I., & Kawata, D. 2018, *MNRAS*, 474, 4112
 Muratov, A. L. & Gnedin, O. Y. 2010, *ApJ*, 718, 1266
 Naidu, R. P., Conroy, C., Bonaca, A., et al. 2020, *ApJ*, 901, 48
 Newberg, H. J., Yanny, B., & Willett, B. A. 2009, *ApJ*, 700, L61
 Nie, J., Tian, H., Li, J., et al. 2022, *ApJ*, 930, 23
 Pawlowski, M. S., Pflamm-Altenburg, J., & Kroupa, P. 2012, *MNRAS*, 423, 1109
 Planck Collaboration, Ade, P. A. R., Aghanim, N., et al. 2016, *A&A*, 586, A132
 Price-Whelan, A. M. 2017, *The Journal of Open Source Software*, 2, 388
 Renaud, F., Agertz, O., & Gieles, M. 2017, *MNRAS*, 465, 3622

- Riley, A. H. & Strigari, L. E. 2020, MNRAS, 494, 983
Rockosi, C. M., Odenkirchen, M., Grebel, E. K., et al. 2002, AJ, 124, 349
Sales, L. V., Helmi, A., Starkenburg, E., et al. 2008, MNRAS, 389, 1391
Shipp, N., Drlica-Wagner, A., Balbinot, E., et al. 2018, ApJ, 862, 114
Tian, H., Liu, C., Luo, C., Xue, X.-X., & Yang, Y. 2024, ApJ, 965, 10
Vasiliev, E. 2019, MNRAS, 482, 1525
Wang, S. & Chen, X. 2019, ApJ, 877, 116
Wilson, J. C., Hearty, F. R., Skrutskie, M. F., et al. 2019, PASP, 131, 055001
Yang, C., Xue, X.-X., Li, J., et al. 2019, ApJ, 880, 65
York, D. G., Adelman, J., Anderson, John E., J., et al. 2000, AJ, 120, 1579
Yuan, Z., Chang, J., Beers, T. C., & Huang, Y. 2020, ApJ, 898, L37
Yuan, Z., Malhan, K., Sestito, F., et al. 2022, ApJ, 930, 103
Zahid, H. J., Geller, M. J., Kewley, L. J., et al. 2013, ApJ, 771, L19
Zinn, R. 1993, in Astronomical Society of the Pacific Conference Series, Vol. 48,
The Globular Cluster-Galaxy Connection, ed. G. H. Smith & J. P. Brodie, 38

Appendix A: space distribution

The coordinates rotation is done with the package `gala`. The two coordinates on the stream $(\alpha_1, \delta_1) = (169.6, -16.9)$ and $(\alpha_2, \delta_2) = (216.9, 11.5)$ are adopted. The left panel in Figure A.1 shows the distribution of the stars in the new coordinate frame. The shadow region represents the selection for the member stars. The right panel represents the number distribution along the latitude ϕ_2 with $-45^\circ < \phi_1 < 65^\circ$. The dashed line represents the fitting results with the latitude dispersion of $\sigma_{\phi_2} = 2^\circ.57$ for a Gaussian distribution $y = A * \text{Gaussian}(\phi_2, \sigma_{\phi_2}) + H$. The background $H = 12.54$.

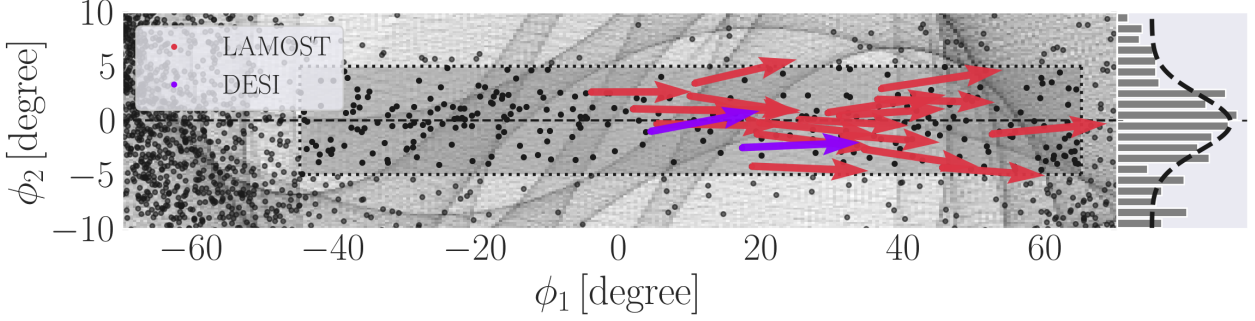


Fig. A.1: The sky distribution of the stars in the new coordinates is showed in the left panel. The shadow region represents the coverage of the new stream with $-45^\circ < \phi_1 < 65^\circ$ and $|\phi_2| < 5^\circ$. The stars with arrows represent the stars with RV from LAMOST (red) and DESI (magenta). The arrows represent the tangential velocities with Solar motion corrected. The right panel shows the number distribution of the stars along the latitude ϕ_2 with longitude $-45^\circ < \phi_1 < 65^\circ$. The dashed line represents the fitting results with a Gaussian distribution.

Appendix B: Distance

Among the selected member candidate stars, there are not classical distance tracers, such as the RR Lyrae stars or blue horizontal stars. The distance is constrained with the isochrone fitting in the color-magnitude diagram distribution of the member candidates, as showed in Figure B.1. Concerning the potential distance gradient, we divide the member candidates into 5 subsamples according to the longitude ϕ_1 with binsize of 22° . The dashed line in each panel represents the magnitude in G -band of 17.6, approximately the red horizontal branch stars with distance modulus of 17.19. The member stars of the globular cluster Pyxis selected from Gaia DR3 according to the position and proper motion are also represented by the blue dots and shifted to the similar distance with the stream.

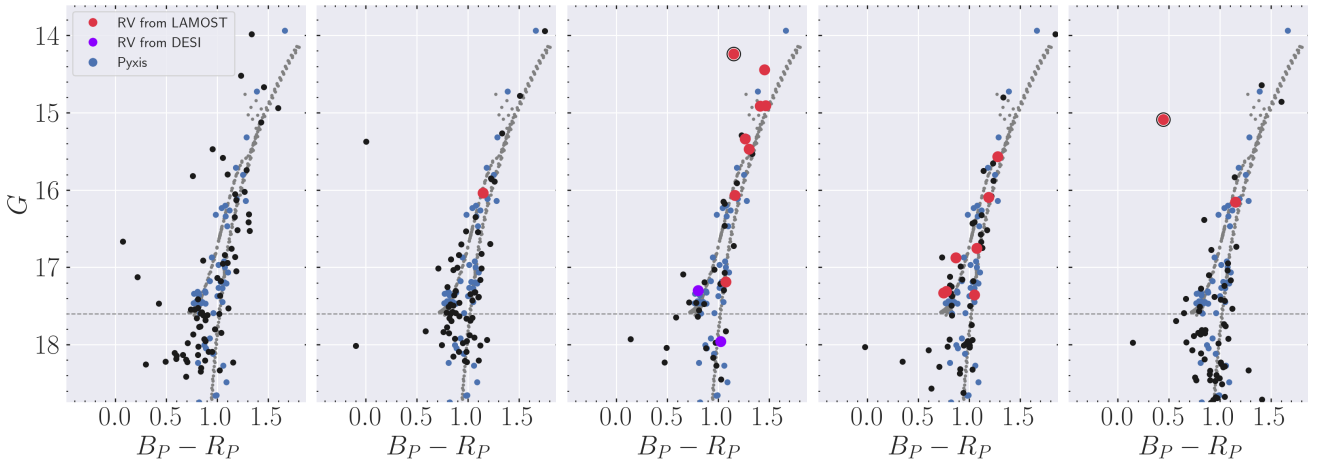


Fig. B.1: The distribution of the member stars in the color magnitude diagram, $B_P - R_P$ versus G within different longitude ϕ_1 ranges. The common stars with LAMOST and DESI are marked with red and magenta dots, respectively. The horizontal dashed line in each panel represents $G = 17.6$ for testing the distance gradient.

Appendix C: Velocity correction

The contribution of the Solar motion to the proper motions of each stars is different because of the different distance and sky position. With distance of each star, this contribution from the Solar motion can be corrected with `gala`. The bottom panel in

Figure C.1 shows the tangential velocities versus the longitude ϕ_1 with the Solar motion corrected. The green symbols represent the average values and the dispersion with different longitude ϕ_1 .

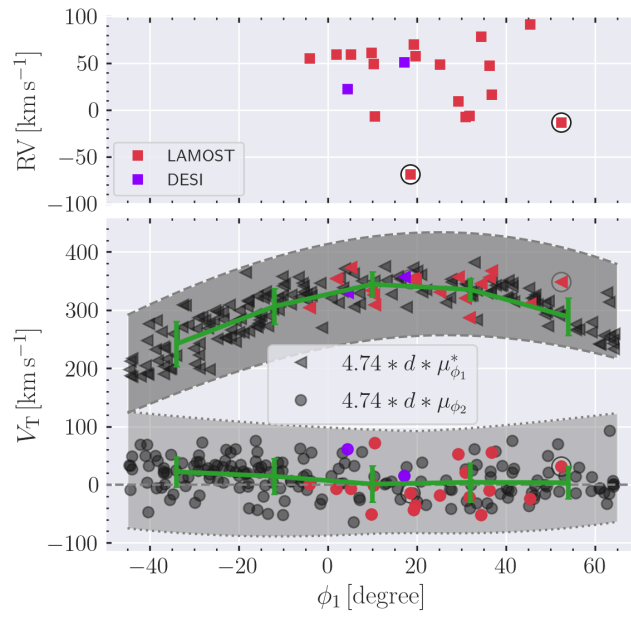


Fig. C.1: Top: The distribution of the radial velocity RV versus the longitude ϕ_1 of all those common stars from LAMOST and DESI, which are represented by the red and magenta squares, respectively. Bottom: The distributions of the tangential velocities V_T versus the longitude ϕ_1 of all the member candidate stars with magnitude $G < 18$. The green lines and the errorbars represent the mean values and the dispersions of the two tangential velocities along the two directions ϕ_1 and ϕ_2 in each subsample with step of $\Delta\phi_1 = 22^\circ$. The shadow regions represent the edges of the tangential velocities caused by the proper motion selection.